

FLOW UNIFORMITY IN A VENTILATED CHAMBER

C.W. Hirt
Flow Science, Inc.
May 1991

DESCRIPTION OF PROBLEM

The problem to be solved is the steady flow pattern of air in a chamber. Flow is generated by a pressure difference existing between an inlet and an outlet port. A schematic of the problem is presented in Fig. 1.

For this test case we assume that the geometry is two dimensional. Furthermore, since preliminary calculations indicate a maximum flow velocity on the order of 15 m/s and the speed of sound in normal air is about 344 m/s, the flow is for all practical purposes incompressible. Although FLOW-3D can model either compressible or incompressible flows, we have assumed incompressibility as being more efficient since it does not require the coupled solution of an energy equation.

Baffles have been used to define the separation between the lower, horizontal inlet channel and the main chamber. In FLOW-3D a baffle is an area blockage at the edge of a control volume but does not occupy any volume. Obstacles, on the other hand, always occupy some volume. In this application the baffles have been given zero porosity, but there are two gaps between them.

One change was made in the original geometry definition of the problem to correspond with the standard capabilities of FLOW-3D. This was to change the low pressure outlet direction from the right side of the flow region to the top. FLOW-3D can only have one pressure (or velocity) condition specified on any given mesh boundary. A simple change could have been introduced into the code (in one subroutine for boundary conditions) to

allow for two different pressure conditions at the right boundary. It was concluded, however, that such a code change would not significantly alter the computed results within the main chamber and was therefore not worth the effort.

As initial conditions, all air in the system was at rest and given a pressure midway between the inlet ($1.01425E+5$ Pa) and the outlet ($1.01225E+5$ Pa). We also set a temperature of 293 K (or 20 C), but this is of no consequence in the present situation because we have assumed incompressibility and no natural convection (i.e., no thermal expansion coefficient for the air).

All quantities in the computations and those shown on the computer-generated plots are in MKS units. A complete input file for the first calculation to be described is given in Fig. 2. This file contains all physical and computational data needed to generate the mesh, geometry (obstacle and baffles), boundary conditions and the type and frequency of output. The file is quite short, which is one measure of how easy and rapidly FLOW-3D can be used.

INVISCID FLOW RESULTS

The first computation was performed assuming no viscosity or turbulence (Euler equations). Because air has a low molecular viscosity and the numerical resolution of the grid, Fig. 3, is insufficient to resolve viscous boundary layers, it is best to treat the problem as one of infinite Reynolds number. In practice, of course, there is always some numerical smoothing associated with the discrete control volumes. To minimize such smoothing, we have selected the second order option available in FLOW-3D (input parameter IORDER=3).

Additionally, because we had no interest in the transient flow leading to steady conditions, we use an acceleration technique to reduce the necessary CPU time. The input defining this acceleration limits the pressure-velocity coupling scheme to one iteration per time cycle (EPSI= $1.0E+6$ and OMEGA=1.0).

The problem was run to a time of $t=0.5$ s and then restarted and run on to $t=1.0$ s. Exact steady-state conditions were not achieved in this time, but the variations in inlet and outlet

velocity were in the 1% to 2% range. Also, the variation of average kinetic energy in the entire computational region was in this same range.

It is interesting to observe that the slight unsteadiness at the end of the calculation can be seen in the velocity vector plots as a shift in the center of the large eddy in the main chamber. This is shown in Fig. 4, which is a composite of vector plots at times 0.85, 0.90, 0.95 and 1.0s (left to right from upper left). The large central eddy seems to slowly move in a clockwise sense, however, the remainder of the flow is essentially unchanged. In particular, the flow near the inlet holes between the baffle plates, the smaller eddy in the lower left corner and the flow at the outlet port are all steady. Based on the average kinetic-energy time history, it is most likely that this slow oscillation will eventually damp out.

An enlarged view of the velocities at $t=1.0$ s is given in Fig. 5A. The maximum velocity is 14.7 m/s and is located in the outlet port.

It should be noted that + signs have been placed at the bases of vectors. This is done so that in problems involving a free surface we can tell where fluid is located even if the velocity magnitude is zero. Arrowheads often make for a "busy" plot and are usually not plotted. For those who can't live without arrowheads see Fig. 5B, which shows an option of the display program provided with FLOW-3D.

It may be concluded from these results that the flow in the main chamber is not uniform because it contains large-scale recirculation. This large-scale motion is caused by the incoming horizontal momentum, which is passed from the inlet channel to the chamber by fluid advection.

TURBULENT FLOW RESULTS

To see how much our assumption of an inviscid flow really affected the flow distribution, a second calculation was performed using a two-equation model of turbulence (the so-called

k-epsilon model). Free-slip walls were still assumed because of lack of boundary layer resolution. We also assumed that the flow entering the inlet was virtually free of turbulence.

The principal influence of turbulence should be the diffusion of the large velocity gradients near the openings in the baffle and possibly a change in secondary eddy flows in the main chamber.

Figure 6 shows the computed velocities at $t=1.0$ s. Comparison with the inviscid results in Fig. 5 shows little difference in the overall flow patterns, but the maximum velocity in the case with turbulence has been reduced from 14.7 m/s to 9.5 m/s.

The reduction in maximum velocity is consistent with a smoother velocity field (i.e., with smaller differences between the high and low velocities). A smoother velocity distribution should mean a reduction in the average kinetic energy of the flow. In fact, this is correct for in the inviscid case the average kinetic energy is about $19.75 \text{ m}^2/\text{s}^2$, while in the turbulent case it is less than $2.64 \text{ m}^2/\text{s}^2$.

A contour plot of the turbulent viscosity is shown in Fig. 7 at $t=1.0$ s. This plot has been restricted in the horizontal direction to only include the width of the chamber (since a maximum viscosity value exists at the outlet that obscures the location of the maximum in the chamber). The large gradient across the baffle near the inlet mostly reflects the lack of turbulence in the inlet channel compared to what develops in the chamber. We see, however, that the viscosity in the main chamber is highest in the lower right corner of the chamber.

At first it seems odd that there should be a relatively large turbulent viscosity in this corner, but upon reflection we note that a nearly zero level of turbulence enters the chamber through the baffle. Turbulence can only arise in the fluid from shearing motions as it flows around in the large recirculating eddy. The lower right corner represents that location farthest from the low turbulence level at the entrance, and hence, where a larger turbulence effect could accumulate.

DEFLECTOR PLATE RESULTS

It appears that the only way to achieve a more uniform flow in the chamber is to prevent the advection of horizontal momentum from the inlet directly into the chamber. One means of doing this is to place flow deflectors in the openings between the baffle plates. For example, Fig. 8 shows a baffle plot where two short, vertical baffle plates have been placed in each opening. These plates should redirect most of the horizontal momentum into the vertical direction and should eliminate the large recirculating eddy.

Figure 9 contains FLOW-3D results for this case and shows that our expectations have been more or less fulfilled. The large recirculation pattern in the previous cases has now been replaced by multiple eddies. A strong jet-like stream flows into the chamber from the left slit, while a relatively small stream enters from the right slit. This is opposite from the previous calculations where the right slit exhibited the strongest flow.

There is an unsteady interaction between the jets exiting the slits. This is best seen from the composite plot in Fig. 10; note the movement of the flow stagnation point along the top boundary.

Further refinement of the flow deflectors would probably improve the uniformity of the flow in the chamber. For example, the incoming flow could be passed through a set of smaller deflectors to produce a fan-shaped flow. Also, it appears that the inlet channel should have a reduced cross section downstream of the first slit so that the flow through the two slits would be more equal.

SUMMARY COMMENTS

Calculations have been completed for the sample ventilation problem using the FLOW-3D computer program. This problem was very easy for FLOW-3D to represent (except for a small change in the orientation of the out-flow port).

One goal of the simulations was to assess the uniformity of flow in the main chamber of the system. Our findings show that the flow is not very uniform because there is a large recirculation eddy established in the chamber. This eddy is generated by the advection of large horizontal momentum from the inlet channel into the chamber.

Because our first calculation was inviscid, there was some concern that the recirculation might have been caused by this limiting approximation. Therefore, a second calculation was performed that included a two-equation turbulence model. This calculation produced the same qualitative flow pattern but with less spatial variation in the velocities.

We can conclude from these two calculations that the non-uniformity in the main chamber is realistic and that it is the result of momentum advection. The only way to eliminate this type of flow pattern is to prevent the direct transfer of horizontal momentum from the inlet to the chamber. One means of doing this is to put flow deflectors in the gaps between the baffles. The deflectors must be designed to give a significant area blockage normal to the horizontal. In this way the flow entering the chamber cannot retain its initial momentum and will be redirected to a more vertical direction, which should prevent the formation of a large-scale recirculating eddy.

To test this idea a third, and final, calculation was performed that had small vertical baffle plates placed in the original inlet gaps. The plates did eliminate the large recirculation pattern but introduced new flow complexities. It is clear from the calculations that further refinement could be made to the deflectors to improve the uniformity of the flow.

The computer time needed to obtain these results is not excessive. For instance, the inviscid case required 3.98 hours of CPU time on a MicroVAX II computer. On a newer DEC 3100 workstation this time would be about 0.4 hours or on a CRAY only a few minutes. The turbulent flow case required 10.56 hours on the MicroVAX or 2.65 times more than that required for the inviscid case. The increase in time reflects an increase in the number of equations to solve and a smaller time-step size, because of the relatively large turbulent viscosity.

Many extensions of this work would be interesting to pursue. Using FLOW-3D we could further explore the consequences of changing the location of the inlets and flow deflectors. Three-dimensional effects could be explored, as could the influence of natural convection. Clearly, this type of computational modeling can provide a considerable amount of useful information to the designer of ventilation systems.

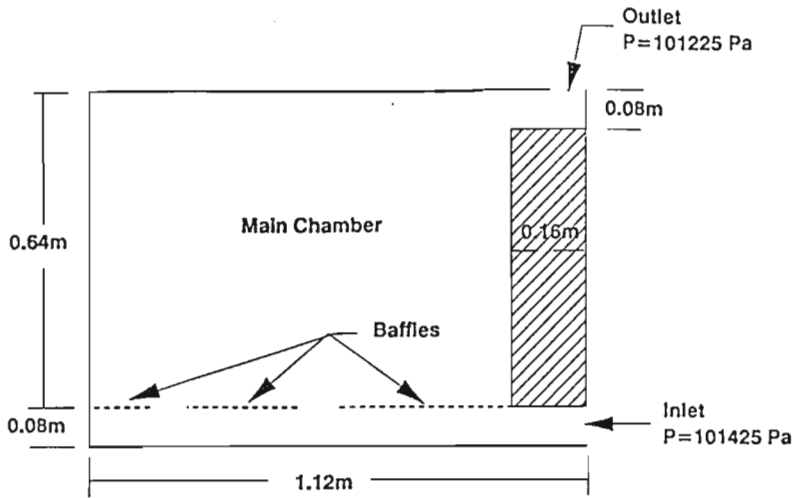


Fig. 1. Schematic of flow region.

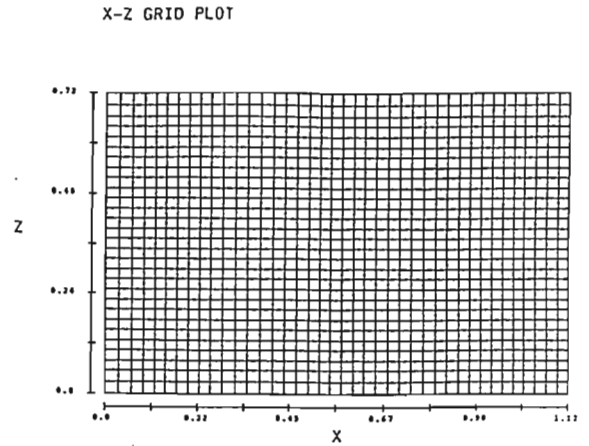


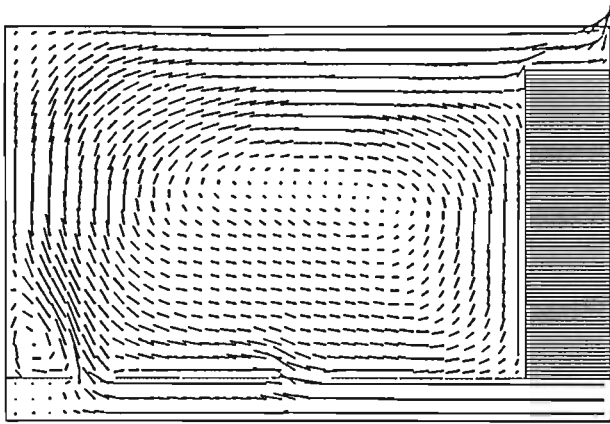
Fig. 2. Computational grid.

Fig. 3. FLOW-3D input file for inviscid case.

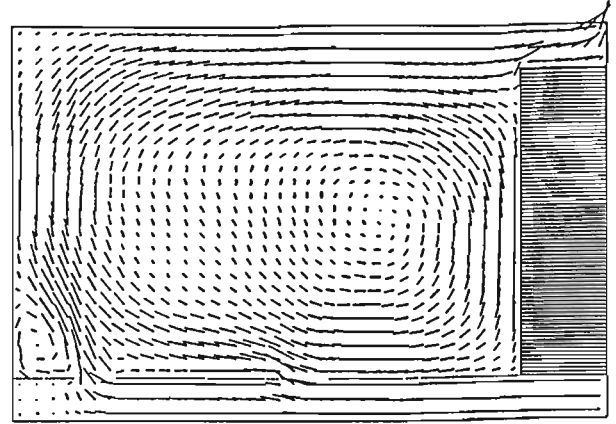
```

AMES -- FLOW UNIFORMITY
$XPUT
REMARK='UNITS: MKS AND KELVIN',          IWSH=0,
ICMPRS=0,      NMAT=1,
PBCTYP=1.0,    IORDER=3,
EPSI=1.0E+6,  OMEGA=1.0,
MUI=0.0,      RHOF=1.2,
WT=5,         PBCT(1,6)=1.01225E+5, TBCT(1,6)=293.0,
WR=5,         PBCT(1,2)=1.01425E+5, TBCT(1,2)=293.0,
WL=2,         WB=2,
TWFIN=0.5,    DELT=0.02,
PRTDT=1.0,    PLTDT=0.05,
IRPR=2,       KTPR=2,
$END
$MESH
NXCELT=40,
PX(2)=0.12,   PX(3)=0.20,   PX(4)=0.52,   PX(5)=0.60,
PX(6)=0.96,   PX(7)=1.12,
NYCELT=1,
PY(2)=1.0,
NZCELT=30,
PZ(2)=0.08,   PZ(3)=0.64,   PZ(4)=0.72,
$END
$OBS
NOBS=1,
IOFO(1,1)=1,
CC(1)=-0.1,   XL(1)=0.96,   ZL(1)=0.08,   ZH(1)=0.64,
$END
$FL
FLHT=1.0,     PRESI=1.01325E+5,
$END
$BF
NBAFS=2,
IBFO(1,1)=1,
BCZ(1)=1.0,   BCC(1)=-0.08,  BXH(1)=0.12,
IBFO(2,1)=2,
BCZ(2)=1.0,   BCC(2)=-0.08,  BXL(2)=0.2,   BXH(2)=0.52,
IBFO(3,1)=3,
BCZ(3)=1.0,   BCC(3)=-0.08,  BXL(3)=0.6,   BXH(3)=0.96,
IBFO(1,2)=4,
BCZ(4)=1.0,   BCC(4)=-0.719, BXH(4)=1.04,
IBFO(2,2)=5,
BCX(5)=1.0,   BCC(5)=-1.119, BZL(5)=0.64,
$END
$TEMP
TEMPI=293.0,
$END
$MOTN
$END
$GRAFIG
NVPLTS=1,
NCPLTS=1,
XLOC(1)=1.1,  YLOC(1)=0.5,   ZLOC(1)=0.04,
XLOC(2)=1.1,  YLOC(2)=0.5,   ZLOC(2)=0.68,
$END
$PARTS
$END

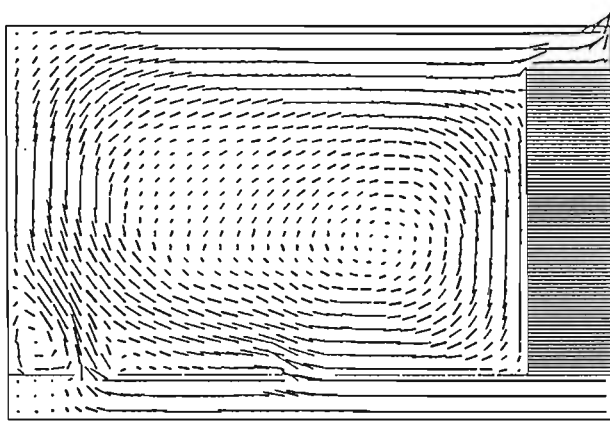
```



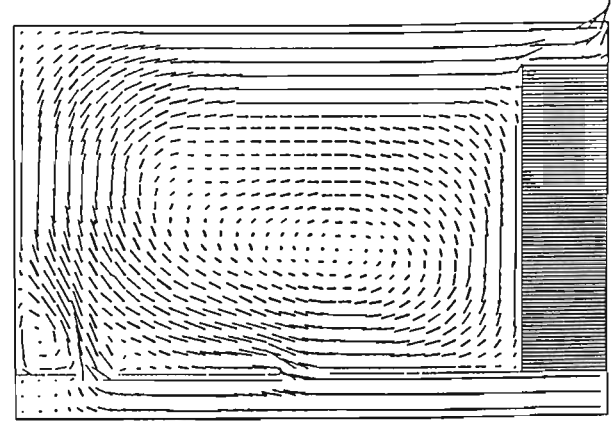
$t=0.85$



$t=0.90$



$t=0.95$



$t=1.0$

Fig. 4. Composite showing small flow configuration changes near end of computation.

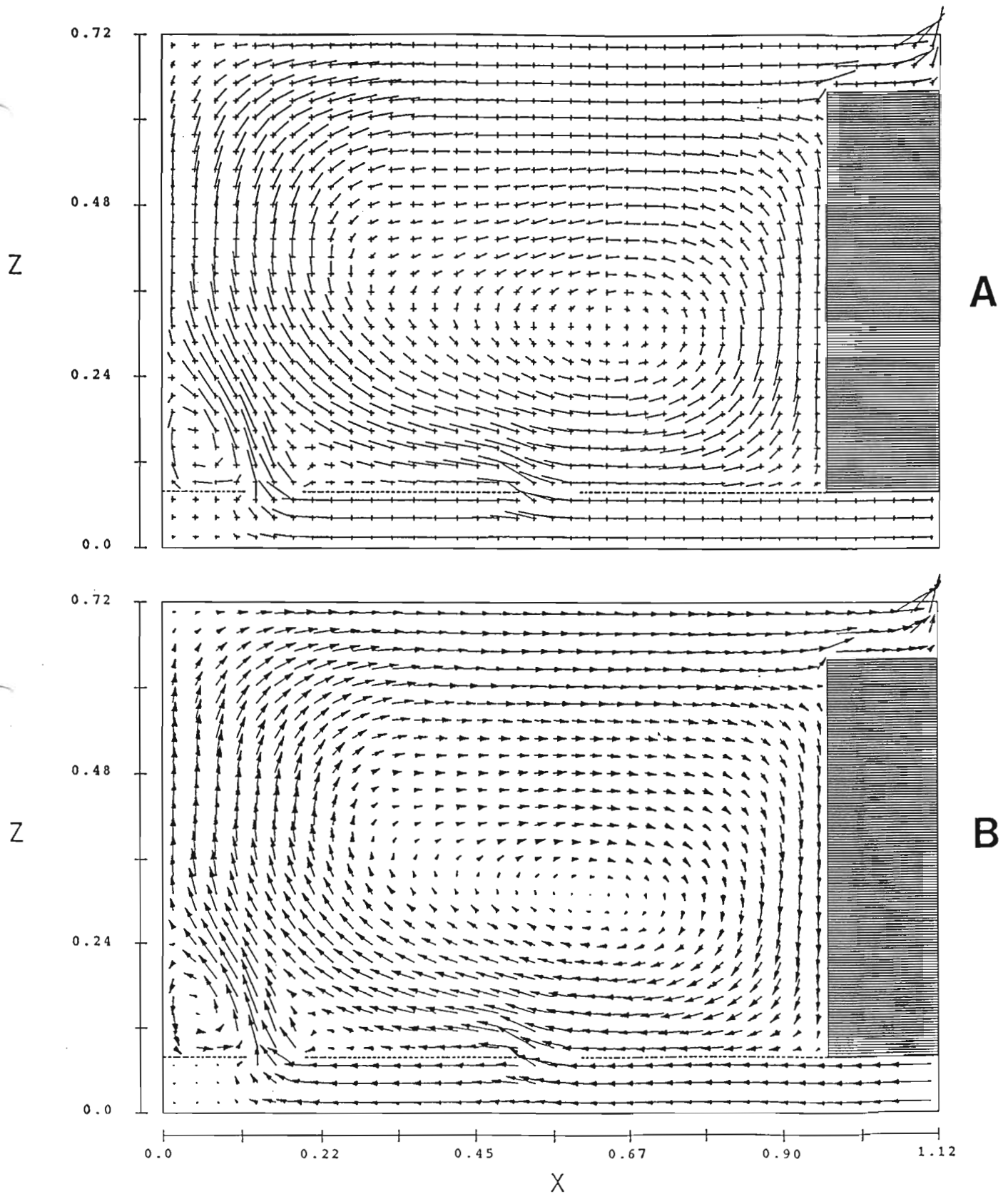


Fig. 5. Inviscid flow field at steady state, (A) without arrowheads and (B) with arrowhead option offered by PLTFSI. Maximum velocity is 14.7 m/s.

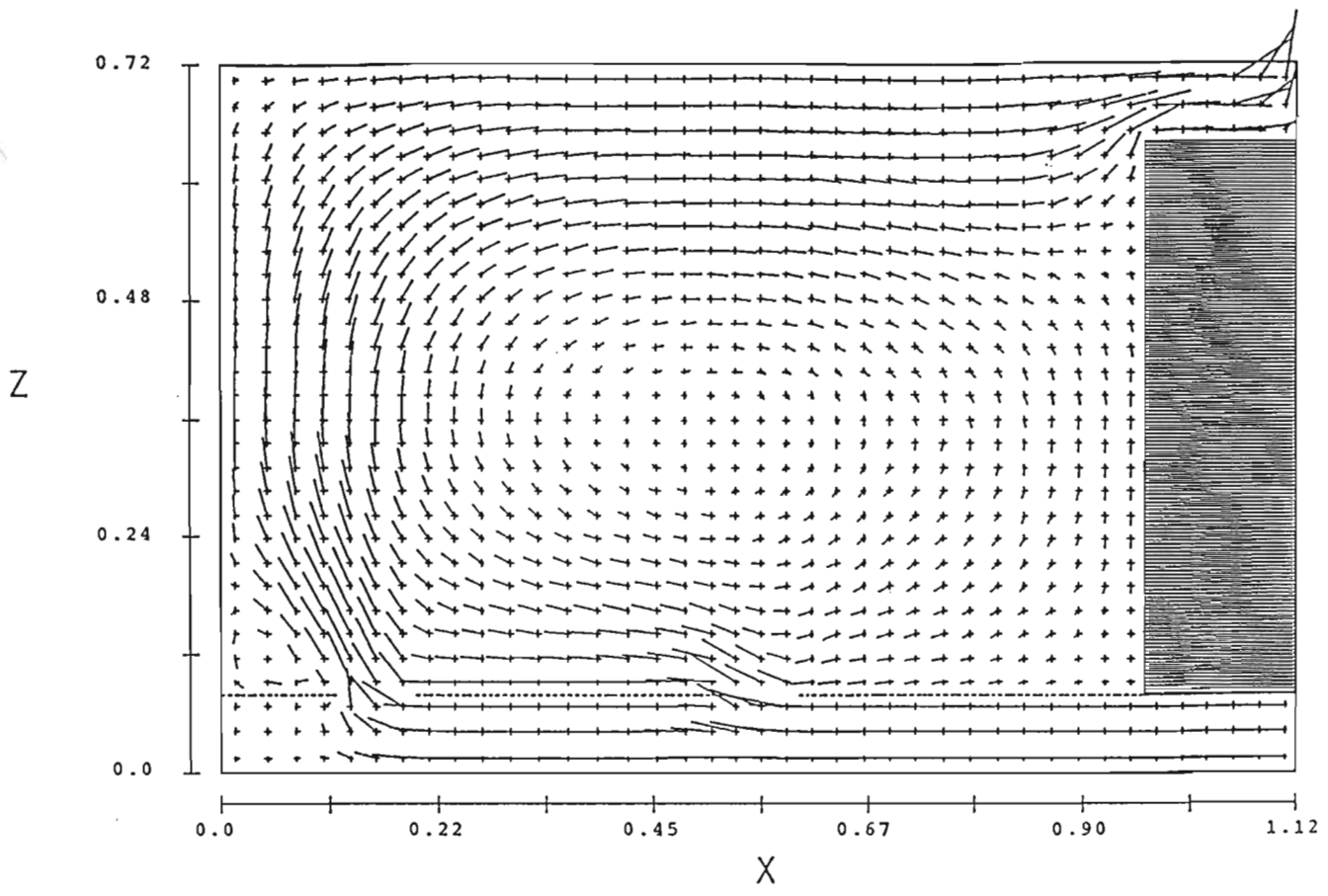


Fig. 6. Turbulent flow field at steady state. Maximum velocity is 9.54 m/s.

TURBULENT VISCOSITY CONTOURS
 (LOW= 1.800E-05 LOW CONTOUR= 6.521E-03)
 (HIGH= 1.301E-01 HIGH CONTOUR= 1.236E-01)

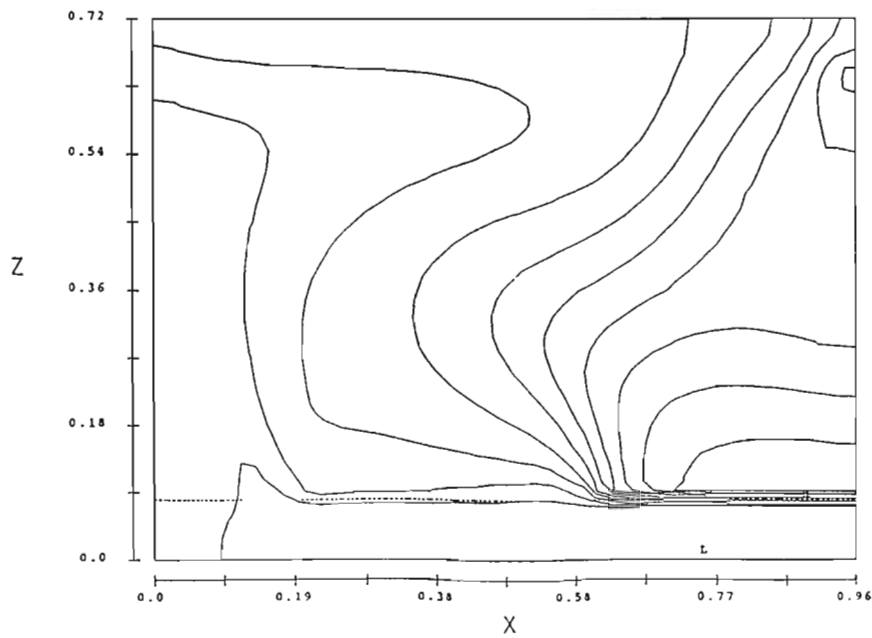


Fig. 7. Turbulent viscosity contours at steady conditions. Right end with obstacle is not shown.

BAFFLE PLOT

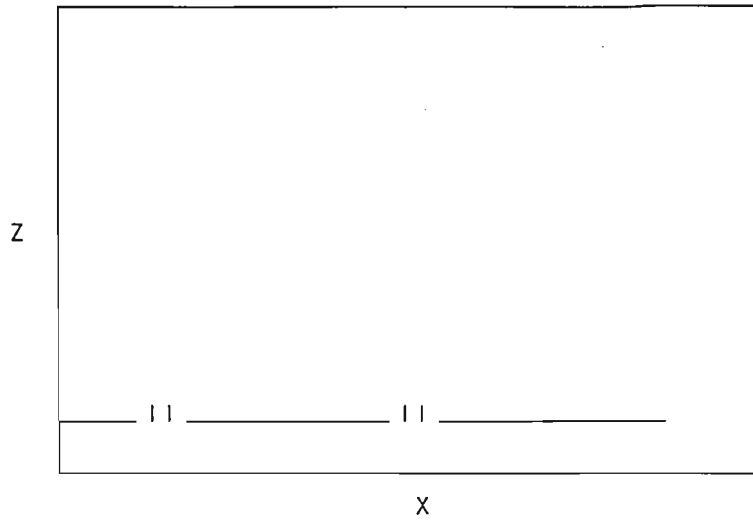


Fig. 8. Baffle plot indicating location of vertical deflector plates.

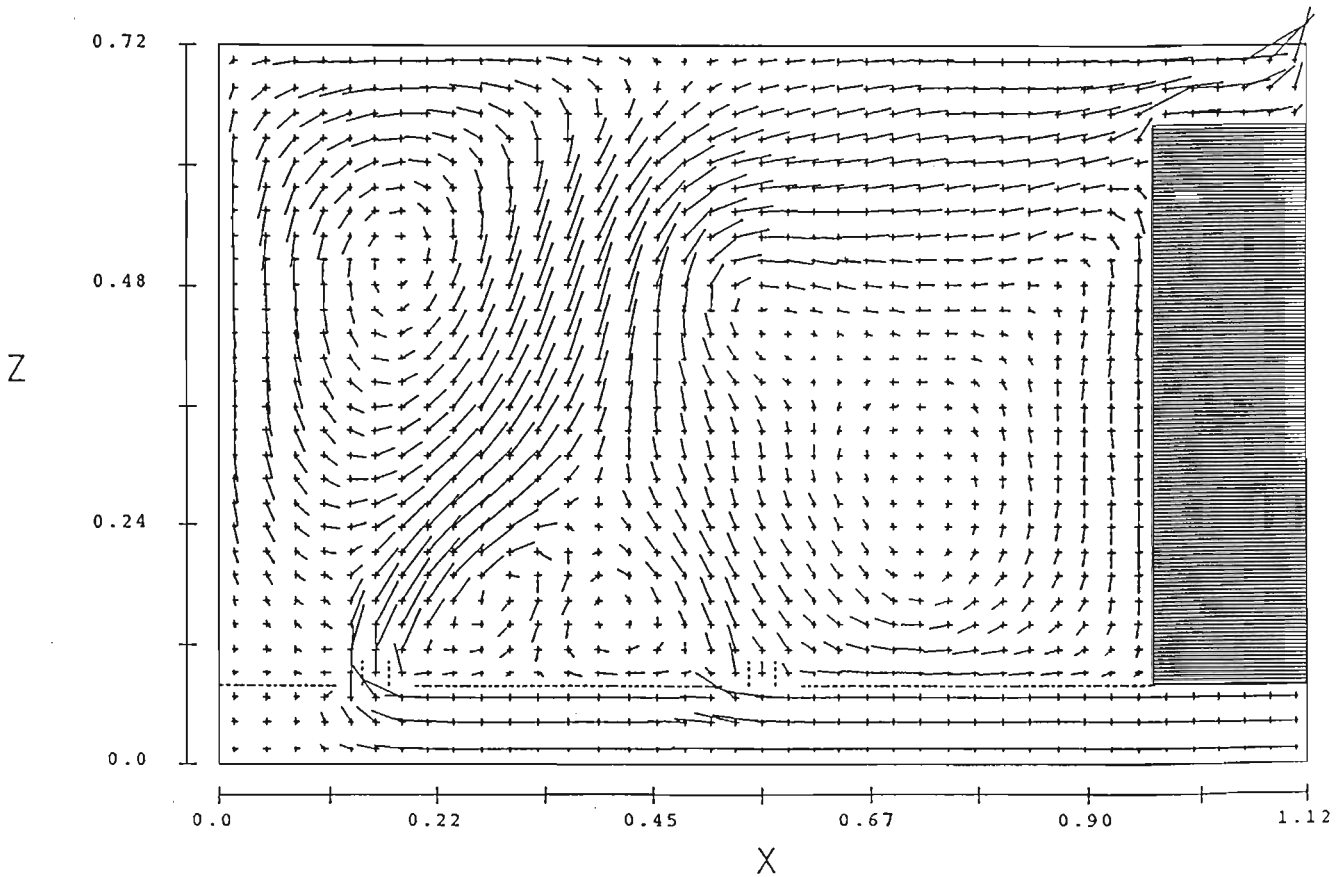
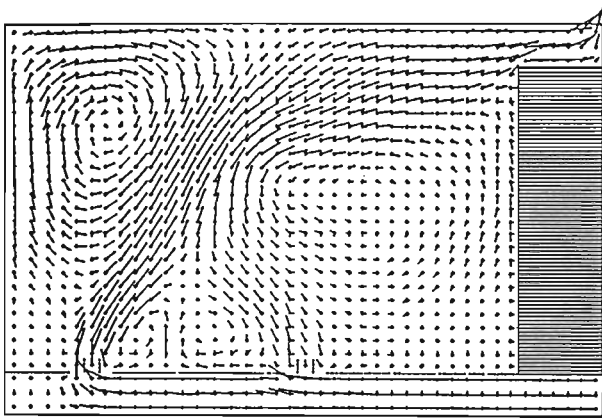
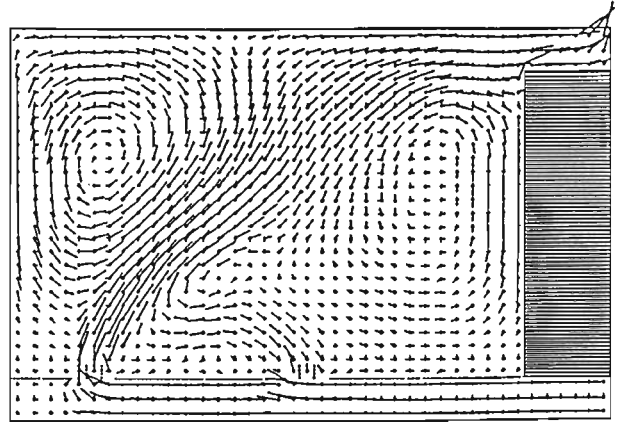


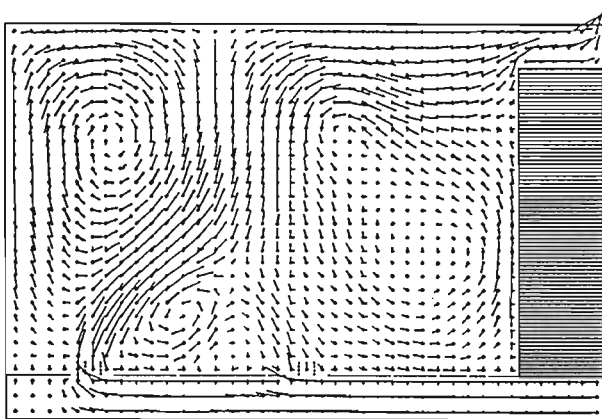
Fig. 9. Deflector-generated flow field at $t=1.0$ s. Maximum velocity is 14.3 m/s.



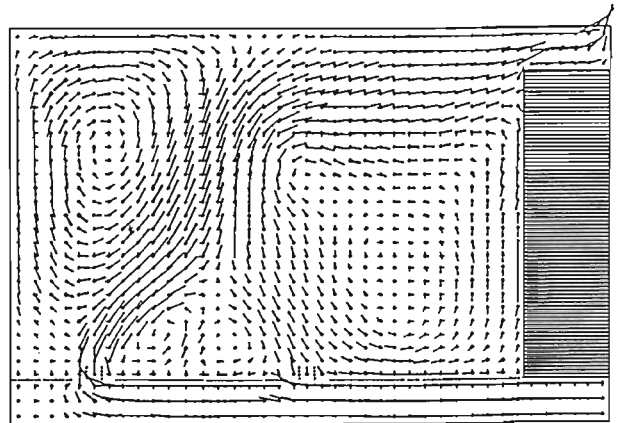
$t=0.7$



$t=0.8$



$t=0.9$



$t=1.0$

Fig. 10. Composite showing unsteady interaction of incoming jets. Times are 0.7, 0.8, 0.9 and 1.0 s.